

Received 27 July 2023

Accepted 19 October 2023

Edited by G. Diaz de Delgado, Universidad de Los Andes Mérida, Venezuela

Keywords: crystal structure; 1,2-azaborinine; boron-nitrogen; zinc; bidentate ligand; Hirshfeld analysis.

CCDC reference: 2302109

Supporting information: this article has supporting information at journals.iucr.org/e

Synthesis and crystal structure of bis(9-mesityl-9,10-dihydro-10-aza-9-borabenz[*h*]quinolinato- $\kappa^2 N^1,N^{10}$)zinc(II)

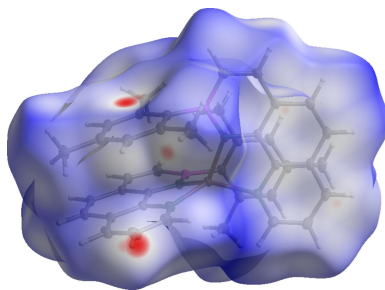
Yannik Appiarius,^{a,b} Pim Puylaert^c and Anne Staubitz^{a,b,*}

^aUniversity of Bremen, Institute for Organic and Analytical Chemistry, 28359 Bremen, Germany, ^bUniversity of Bremen, MAPEX Center for Materials and Processes, 28359 Bremen, Germany, and ^cUniversity of Bremen, Institute for Inorganic Chemistry and Crystallography, 28359 Bremen, Germany. *Correspondence e-mail: staubitz@uni-bremen.de

The title compound, $[Zn(C_{20}H_{18}BN_2)_2]$ (**ZnL₂**), is an overall uncharged chelate that consists of two units of an NH-deprotonated 10-aza-9-borabenz[*h*]quinoline ligand (*L*) per Zn^{II} center. It was synthesized in two steps by treating the protonated ligand **HL** with lithium bis(trimethylsilyl)amide and further conversion with diethylzinc. Its asymmetric unit comprises one **ZnL** fragment; the molecule is completed by application of inversion symmetry at Zn. Due to the fourfold coordination with nitrogen atoms, the zinc(II) ion is located in a distorted tetrahedral environment. Besides the relatively short N–Zn bonds, **ZnL₂** is characterized by the significant protrusion of the central ion from the plane of the ligand backbone. The crystal structure is consolidated by intra- and intermolecular π – π stacking interactions, while the polarized B–N bond is barely involved in any close atom contacts.

1. Chemical context

1,2-Azaborinine is an aromatic six-membered ring that consists of a polar boron-nitrogen unit and a butadienyl moiety, making it an isoelectronic congener of benzene. Its strikingly similar geometry in conjunction with a significantly altered electron distribution has promoted research on mono- and polycyclic aromatic hydrocarbons (PAHs) with a BN substitution pattern. Several studies highlighted the BN-induced tailored adjustment of chemical, physical and optical properties, enabling the application of such heteroaromatics for instance as white-emitting layers in organic light-emitting diodes (Hoffmann *et al.*, 2021), as reversible hydrogen storage materials (Campbell *et al.*, 2010) or as building blocks in pharmaceuticals with increased bioavailability (Zhao *et al.*, 2017). Relatively few reports made use of the selectively deprotonable NH group ($pK_a \approx 24$) to introduce electrophilic functional groups or metal atoms (Pan *et al.*, 2004; Lamm *et al.*, 2011; Baggett & Liu, 2017; Lindl *et al.*, 2023).



OPEN ACCESS

Published under a CC BY 4.0 licence

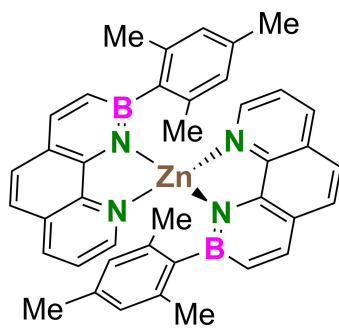


Table 1Selected geometric parameters (\AA , $^\circ$).

Zn1–N1	1.9606 (10)	N2–C2	1.3660 (16)
Zn1–N2	2.0527 (10)	N2–C3	1.3316 (17)
N1–C1	1.3580 (14)	C12–B1	1.5896 (18)
N1–B1	1.4245 (17)	C11–B1	1.5315 (19)
N1 ⁱ –Zn1–N1	118.68 (6)	N1–Zn1–N2	84.72 (4)
N1 ⁱ –Zn1–N2	122.48 (4)	N2–Zn1–N2 ⁱ	128.26 (6)
Zn1–N1–C1–C9	166.76 (9)	Zn1–N1–B1–C12	20.10 (16)
Zn1–N1–C1–C2	−14.38 (13)	Zn1–N1–B1–C11	−163.25 (9)

Symmetry code: (i) $-x + 1, y, -z + \frac{3}{2}$.

In a previous study (Appiarus *et al.*, 2021), a BN-substituted benzo[*h*]quinoline (**HL**), containing one 1,2-azaborininyl- and one pyridyl subunit with both nitrogen atoms beneficially preorganized for chelation was presented. In the context of this communication, we report on the synthesis and crystal structure of the 2:1 coordination complex of ligand **L** with zinc(II).

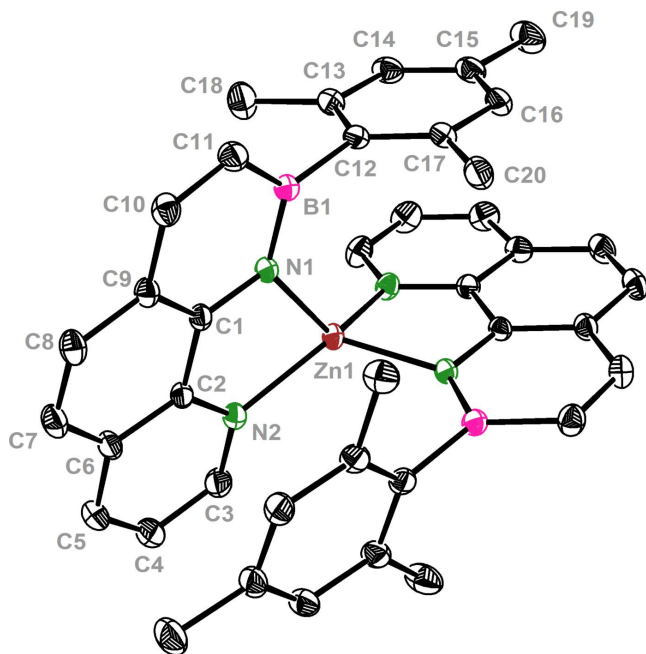
2. Structural commentary

The molecular structure of the title compound ($\text{C}_{40}\text{H}_{36}\text{B}_2\text{N}_4\text{Zn}$, **ZnL₂**) is illustrated in Fig. 1. The coordination complex crystallizes in the monoclinic *C*2/c centrosymmetric space group with one zinc(II) cation and one ligand molecule in the asymmetric unit, being completed by the application of inversion symmetry at Zn^{II}. The latter is four-fold coordinated by two types of N donors, namely the azaborinine and pyridine subunits comprised in the BN-benzo[*h*]quinoline. This results in a significantly distorted tetrahedral

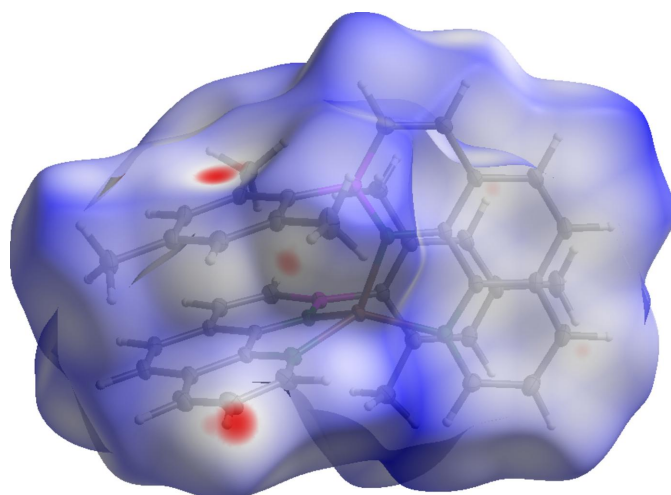
configuration [bond angle N1–Zn1–N2 84.72 (4) $^\circ$; all other N–Zn–N bond angles $> 118^\circ$, see Table 1]. The bond lengths within the 1,2-azaborinine motif of the ligand [B1–N1: 1.4245 (17) \AA , B1–C11: 1.5315 (19) \AA , N1–C1: 1.3580 (14) \AA] are in characteristic ranges (Paetzold *et al.*, 2004; Pan *et al.*, 2009), confirming electron delocalization and an elevated aromatic character. The N–Zn bond lengths [N1–Zn1: 1.9606 (10) \AA , N2–Zn1: 2.0527 (10) \AA] are in excellent agreement with bis(2-(2'-pyridyl)pyrrolyl)zinc [$\text{N}_{\text{pyrrole}}\text{-Zn}$ 1.9513 (18) \AA , $\text{N}_{\text{pyridine}}\text{-Zn}$ 2.0444 (18) \AA ; Wang *et al.*, 2009], supporting the electronic similarities of 1,2-azaborinine and pyrrole (Davies *et al.*, 2017). This contrasts with zinc complexes involving the geometrically similar but uncharged 1,10-phenanthroline ligand ($\text{N}_{\text{pyridine}}\text{-Zn}$ 2.13–2.20 \AA) with higher coordination numbers of the central ion. All aromatic rings within the BN-PAH ligand are close to planar, with an average torsion angle of 2.2 $^\circ$ and a maximum deviation of an atom from the mean aromatic plane of 0.0217 (8) \AA . In contrast, the Zn^{II} ion is located 0.365 (2) \AA out of the mean N1–C1–C2–N2 plane and points in the direction of the mesityl ring of the second ligand unit. The 1,2-azaborinine motif and the attached planar mesityl group [maximum deviation from the mean aromatic plane: 0.0125 (9) \AA] are oriented almost perpendicularly to each other, with an angle between their mean planes of 79.41 (4) $^\circ$.

3. Supramolecular features and Hirshfeld surface analysis

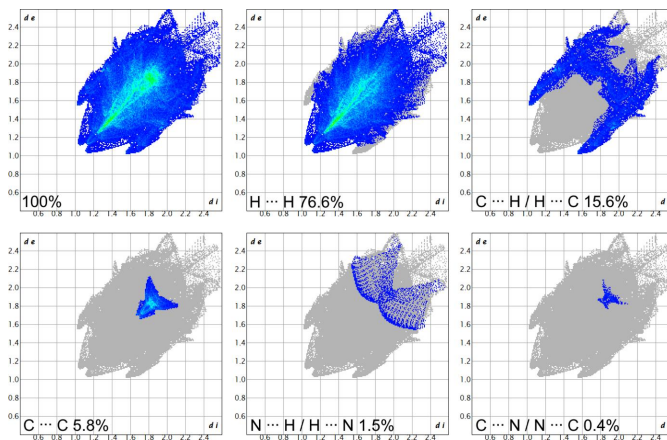
A Hirshfeld surface (Hirshfeld, 1977, Fig. 2) and the respective two-dimensional fingerprint plots (Fig. 3) were generated using *CrystalExplorer21.5* (Spackman *et al.*, 2021) to analyze the intermolecular interactions. No close atom contacts involving the boron and zinc heteroatoms and a negligible participation of the nitrogen atom (N···H: 1.5%, C···N: 0.4%) were found. Therefore, the intermolecular interactions were almost exclusively caused by van der Waals forces

**Figure 1**

Molecular structure of **ZnL₂** with atom labeling. The image was generated with *ORTEP-3 for Windows* (Farrugia, 2012). Non-hydrogen atoms as displacement ellipsoids drawn at the 50% probability level. Hydrogen atoms were omitted for clarity. [Symmetry code: (i) $-x + 1, y, -z + \frac{3}{2}$].

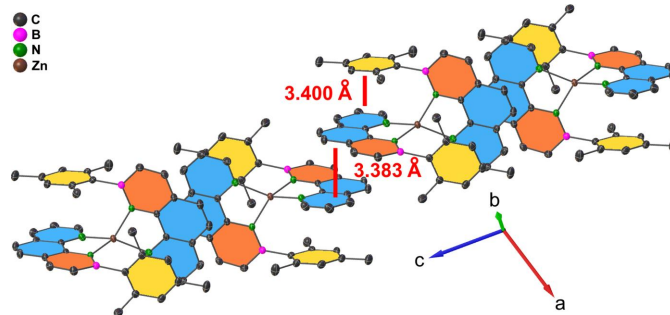
**Figure 2**

Hirshfeld surface of **ZnL₂**, mapped over d_{norm} in the range between −0.1418 (red) and +1.6402 (blue).

**Figure 3**

Two-dimensional fingerprint plots, showing the contributions of the individual elements in close atom contacts.

involving carbon and hydrogen. In particular, close H···H contacts and aromatic interactions dominate the overall intermolecular interactions in a crystal. The ‘wings’ at the top left ($d_i \approx 1.05 \text{ \AA}$ and $d_e \approx 1.60 \text{ \AA}$) and their pseudo-symmetrical counterparts at the bottom right of the two-dimensional fingerprint plot correspond to C—H···π interactions. These are also mapped by several red spots on the Hirshfeld surface (Spackman & McKinnon, 2002). Moreover, considerable π—π stacking interactions are apparent by the light coloring of the Hirshfeld surface around the PAH backbone and intense C···C contacts (5.8%). The crystal packing shows that each aromatic ligand has one ligand unit of another molecule in close proximity, so that pairs of almost parallel but slightly displaced sheets in two dimensions result (Fig. 4). In particular, the phenyl and pyridyl subunits of neighboring molecules show a significant overlap, with an offset of only 1.181 (2) Å and a minimum interplanar distance of 3.3826 (13) Å. On the other hand, the PAH scaffolds and the mesityl π-planes of the inverse ligand units are aligned almost coplanar [mesityl-pyridine interplanar angle: 1.46 (5)°] with a similarly small minimum interplanar distance [3.3996 (10) Å]. Therefore, intramolecular π—π stacking contributes significantly to the overall stabilizing forces. We assume that the discussed, unusual off-plane position of the

**Figure 4**

Section of the crystal packing, showing the π—π stacking interactions propagating in two dimensions. BN rings are shown in orange, mesityl rings in yellow, phenyl and pyridyl rings in blue.

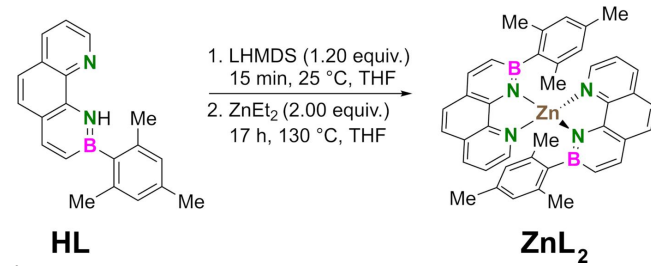
zinc ion and the increased angle between the mean mesityl plane and the B1—C12 bond [7.93 (8)°] also derives from this favorable stacking geometry.

4. Database survey

A survey of the Cambridge Structural Database (WebCSD version 1.9.32, accessed in July 2023; Groom *et al.*, 2016) revealed that 654 crystal structures of six-membered carbocycles with 1-aza-2-bora substitution patterns have been reported. Among these, 101 structures comprising *B*-mesityl substituents have been deposited, which involves aromatic 1,2-azaborinines for the most part. The crystal structures of 13 compounds with 1,2-azaborinine substructures and nitrogen–metal bonds have been published, of which different lithium solvates as well as potassium, beryllium, aluminum, gallium and tin complexes are included in one publication (Lindl *et al.*, 2023). Moreover, one study describes several complexes of a bidentate ligand with aluminum (Appiarus *et al.*, 2023). However, there are only three reports of 1,2-azaborinines with N-transition-metal bonds, including zirconium (refcode JIZQEP; Pan *et al.*, 2008), ruthenium (refcode DOXBEY; Pan *et al.*, 2008) and iridium (refcode NEZXAV; Baschieri *et al.*, 2023). Also, the structure of a 6-pyridyl-1,2-azaborinine has been reported, which is structurally similar to **HL** and was used for the preparation of a dimesitylboron complex (refcode WUGMIW; Baggett *et al.*, 2015). The search query for coordination complexes of zinc with 1,2-azaborinine ligands did not yield any results.

5. Synthesis and crystallization

The synthesis of **ZnL₂** is shown in Fig. 5. Under argon at 298 K, 9,10-dihydro-9-mesityl-10-aza-9-borabenz[*h*]quino-line (**HL**, 29.8 mg, 100 μmol, 1.00 equiv., prepared according to Appiarus *et al.*, 2021) was dissolved in THF (1.5 mL). A solution of lithium bis(trimethylsilyl)amide (1.0 M in THF, 120 μL, 1.20 equiv.) was added, before a solution of diethylzinc (15% *w/w* in hexanes, 230 μL, 2.00 equiv.) was added *via* a syringe. The mixture was heated to 428 K for 17 h while stirring. In a glove box, the volatiles were removed under reduced pressure. The residue was extracted with *n*-hexane (3 × 2 mL) and the solvent was removed. The crude product was dissolved in THF (500 μL) and *n*-hexane was allowed to diffuse into this solution over the course of 3 d. The light-yellow product (6.4 mg, 19%) was obtained as air-sensitive crystals suitable

**Figure 5**

Reaction scheme for the synthesis of **ZnL₂**.

Table 2
Experimental details.

Crystal data	
Chemical formula	[Zn(C ₂₀ H ₁₈ BN ₂) ₂]
M_r	659.72
Crystal system, space group	Monoclinic, C2/c
Temperature (K)	100
a, b, c (Å)	20.0425 (14), 9.8589 (6), 17.1167 (9)
β (°)	105.172 (4)
V (Å ³)	3264.3 (4)
Z	4
Radiation type	Mo $K\alpha$
μ (mm ⁻¹)	0.79
Crystal size (mm)	0.24 × 0.12 × 0.09
Data collection	
Diffractometer	Bruker APEXII CCD
Absorption correction	Multi-scan (<i>SADABS</i> ; Krause <i>et al.</i> , 2015)
T_{\min}, T_{\max}	0.677, 0.747
No. of measured, independent and observed [$I > 2\sigma(I)$] reflections	95271, 6577, 5466
R_{int}	0.084
(sin θ/λ) _{max} (Å ⁻¹)	0.784
Refinement	
$R[F^2 > 2\sigma(F^2)]$, $wR(F^2)$, S	0.036, 0.097, 1.06
No. of reflections	6577
No. of parameters	216
H-atom treatment	H-atom parameters constrained
$\Delta\rho_{\max}, \Delta\rho_{\min}$ (e Å ⁻³)	0.52, -0.40

Computer programs: *APEX2* and *SAINT* (Bruker, 2016), *SHELXT2018/2* (Sheldrick, 2015a), *SHELXL2018/3* (Sheldrick, 2015b), *OLEX2* (Dolomanov *et al.*, 2009), *ORTEP-3* for Windows (Farrugia, 2012), and *publCIF* (Westrip, 2010).

for X-ray diffraction analysis by repeating this process twice. **¹H NMR** (600 MHz, THF-*d*₈): δ = 8.37–8.32 (*m*, 4H, C3-H + C5-H), 8.07 (*d*, ³*J* = 11.0 Hz, 2H, C10-H), 7.79 (*d*, ³*J* = 8.7 Hz, 2H, C8-H), 7.38–7.35 (*m*, 2H, C4-H), 7.33 (*d*, ³*J* = 8.7 Hz, 2H, C7-H), 6.90 (*d*, ³*J* = 11.0 Hz, 2H, C11-H), 6.04 (*s*, 2H, C14-H), 5.61 (*s*, 2H, C16-H), 1.83 (*s*, 6H, C19-H), 1.79 (*s*, 6H, C18-H), 1.40 (*s*, 6H, C20-H) ppm. **¹³C{¹H} NMR** (151 MHz, THF-*d*₈): δ = 147.3 (C3), 145.8 (C1), 143.3 (C2), 143.0 (C10), 139.2 (C17), 139.2 (C5), 139.1 (C13), 134.8 (C15), 134.5 (C11), 131.2 (C8), 129.0 (C6), 127.1 (C14), 126.4 (C16), 126.1 (C9), 122.3 (C4), 116.1 (C7), 24.0 (C18), 23.8 (C20), 21.3 (C19) ppm. **¹¹B{¹H} NMR** (193 MHz, THF-*d*₈): δ = 38.6 ppm. **MS** (EI): *m/z* 658.3 (3%) [ZnL₂]⁺, 298.2 (100%) [HL]⁺. **HR-MS** (EI): *m/z* calculated for C₄₀H₃₆B₂N₄Zn⁺ 658.24259, found 658.24253 (Dev.: 0.06 mu, 0.09 ppm). **UV/Vis**: λ_{abs} = 296, 343, 358 nm. **Fluorescence**: λ_{fl} = 488 nm (λ_{exc} = 350 nm). Further experimental details can be found in the Supporting Information.

6. Refinement

Crystal data, data collection and structure refinement details are summarized in Table 2. Hydrogen atoms were positioned geometrically and refined using a riding model with C—H bond lengths of 0.95 Å (C—H) or 0.98 Å (C—H₃). Isotropic displacement parameters (*U*_{iso}) of these H atoms were fixed to 1.2 (C—H) or 1.5 (C—H₃) of the values of the parent carbon

atoms. Idealized methyl groups (C18—H₃, C19—H₃, C20—H₃) were allowed to rotate.

Funding information

Funding for this research was provided by: Central Research Development Fund of the University of Bremen (postdoctoral fellowship to Pim Puylaert).

References

- Appiarius, Y., Puylaert, P., Werthschütz, J., Neudecker, T. & Staubitz, A. (2023). *Inorganics* **11**, 295.
- Appiarius, Y., Stauch, T., Lork, E., Rusch, P., Bigall, N. C. & Staubitz, A. (2021). *Org. Chem. Front.* **8**, 10–17.
- Baggett, A. W. & Liu, S.-Y. (2017). *J. Am. Chem. Soc.* **139**, 15259–15264.
- Baggett, A. W., Vasiliu, M., Li, B., Dixon, D. A. & Liu, S.-Y. (2015). *J. Am. Chem. Soc.* **137**, 5536–5541.
- Baschieri, A., Aleotti, F., Matteucci, E., Sambri, L., Mancinelli, M., Mazzanti, A., Leoni, E., Armaroli, N. & Monti, F. (2023). *Inorg. Chem.* **62**, 2456–2469.
- Bruker (2016). *APEX2* and *SAINT*. Bruker AXS Inc., Madison Wisconsin, USA.
- Campbell, P. G., Zakharov, L. N., Grant, D. J., Dixon, D. A. & Liu, S.-Y. (2010). *J. Am. Chem. Soc.* **132**, 3289–3291.
- Davies, G. H. M., Jouffroy, M., Sherafat, F., Saeednia, B., Howshall, C. & Molander, G. A. (2017). *J. Org. Chem.* **82**, 8072–8084.
- Dolomanov, O. V., Bourhis, L. J., Gildea, R. J., Howard, J. A. K. & Puschmann, H. (2009). *J. Appl. Cryst.* **42**, 339–341.
- Farrugia, L. J. (2012). *J. Appl. Cryst.* **45**, 849–854.
- Groom, C. R., Bruno, I. J., Lightfoot, M. P. & Ward, S. C. (2016). *Acta Cryst. B* **72**, 171–179.
- Hirshfeld, F. L. (1977). *Theor. Chim. Acta* **44**, 129–138.
- Hoffmann, J., Geffroy, B., Jaques, E., Hissler, M. & Staubitz, A. (2021). *J. Mater. Chem. C* **9**, 14720–14729.
- Krause, L., Herbst-Irmer, R., Sheldrick, G. M. & Stalke, D. (2015). *J. Appl. Cryst.* **48**, 3–10.
- Lamm, A. N., Garner, E. B. III, Dixon, D. A. & Liu, S.-Y. (2011). *Angew. Chem. Int. Ed.* **50**, 8157–8160.
- Lindl, F., Lamprecht, A., Arrowsmith, M., Khitro, E., Rempel, A., Dietz, M., Wellnitz, T., Bélanger-Chabot, G., Stoy, A., Paprocki, V., Prieschl, D., Lenczyk, C., Ramler, J., Lichtenberg, C. & Braunschweig, H. (2023). *Chem. A Eur. J.* **29**, e202203345.
- Paetzold, P., Stanescu, C., Stubenrauch, J. R., Bienmüller, M. & Englert, U. (2004). *Z. Anorg. Allg. Chem.* **630**, 2632–2640.
- Pan, J., Kampf, J. W. & Ashe, A. J. (2004). *Organometallics* **23**, 5626–5629.
- Pan, J., Kampf, J. W. & Ashe, A. J. (2008). *Organometallics* **27**, 1345–1347.
- Pan, J., Kampf, J. W. & Ashe, A. J. (2009). *Organometallics* **28**, 506–511.
- Sheldrick, G. M. (2015a). *Acta Cryst. A* **71**, 3–8.
- Sheldrick, G. M. (2015b). *Acta Cryst. C* **71**, 3–8.
- Spackman, M. A. & McKinnon, J. J. (2002). *CrystEngComm* **4**, 378–392.
- Spackman, P. R., Turner, M. J., McKinnon, J. J., Wolff, S. K., Grimwood, D. J., Jayatilaka, D. & Spackman, M. A. (2021). *J. Appl. Cryst.* **54**, 1006–1011.
- Wang, H., Zeng, Y., Ma, J. S., Fu, H., Yao, J., Mikhaleva, A. I. & Trofimov, B. A. (2009). *Chem. Commun.* pp. 5457–5459.
- Westrip, S. P. (2010). *J. Appl. Cryst.* **43**, 920–925.
- Zhao, P., Nettleton, D. O., Karki, R. G., Zécri, F. J. & Liu, S.-Y. (2017). *ChemMedChem*, **12**, 358–361.

supporting information

Acta Cryst. (2023). E79, 1063-1066 [https://doi.org/10.1107/S2056989023009192]

Synthesis and crystal structure of bis(9-mesityl-9,10-dihydro-10-aza-9-borabenz[*h*]quinolinato- κ^2N^1,N^{10})zinc(II)

Yannik Apparius, Pim Puylaert and Anne Staubitz

Computing details

Data collection: *APEX2* (Bruker, 2016); cell refinement: *SAINT* (Bruker, 2016); data reduction: *SAINT* (Bruker, 2016); program(s) used to solve structure: *SHELXT2018/2* (Sheldrick, 2015a); program(s) used to refine structure: *SHELXL2018/3* (Sheldrick, 2015b); molecular graphics: Olex2 1.5 (Dolomanov *et al.*, 2009), *ORTEP-3 for Windows* (Farrugia, 2012); software used to prepare material for publication: *publCIF* (Westrip, 2010).

Bis(9-mesityl-9,10-dihydro-10-aza-9-borabenz[*h*]quinolinato- κ^2N^1,N^{10})zinc(II)

Crystal data

[Zn(C ₂₀ H ₁₈ BN ₂) ₂]	<i>F</i> (000) = 1376
<i>M_r</i> = 659.72	<i>D_x</i> = 1.342 Mg m ⁻³
Monoclinic, <i>C2/c</i>	Mo <i>Kα</i> radiation, λ = 0.71073 Å
<i>a</i> = 20.0425 (14) Å	Cell parameters from 9897 reflections
<i>b</i> = 9.8589 (6) Å	θ = 2.8–33.4°
<i>c</i> = 17.1167 (9) Å	μ = 0.79 mm ⁻¹
β = 105.172 (4)°	<i>T</i> = 100 K
<i>V</i> = 3264.3 (4) Å ³	Irregular, light yellow
<i>Z</i> = 4	0.24 × 0.12 × 0.09 mm

Data collection

Bruker APEXII CCD	6577 independent reflections
diffractometer	5466 reflections with $I > 2\sigma(I)$
φ and ω scans	R_{int} = 0.084
Absorption correction: multi-scan	$\theta_{\text{max}} = 33.9^\circ$, $\theta_{\text{min}} = 2.8^\circ$
(SADABS; Krause <i>et al.</i> , 2015)	$h = -31 \rightarrow 31$
$T_{\text{min}} = 0.677$, $T_{\text{max}} = 0.747$	$k = -15 \rightarrow 15$
95271 measured reflections	$l = -26 \rightarrow 26$

Refinement

Refinement on F^2	Hydrogen site location: inferred from
Least-squares matrix: full	neighbouring sites
$R[F^2 > 2\sigma(F^2)]$ = 0.036	H-atom parameters constrained
$wR(F^2)$ = 0.097	$w = 1/[\sigma^2(F_o^2) + (0.0416P)^2 + 3.4887P]$
S = 1.06	where $P = (F_o^2 + 2F_c^2)/3$
6577 reflections	$(\Delta/\sigma)_{\text{max}} < 0.001$
216 parameters	$\Delta\rho_{\text{max}} = 0.52$ e Å ⁻³
0 restraints	$\Delta\rho_{\text{min}} = -0.40$ e Å ⁻³
Primary atom site location: dual	

Special details

Geometry. All esds (except the esd in the dihedral angle between two l.s. planes) are estimated using the full covariance matrix. The cell esds are taken into account individually in the estimation of esds in distances, angles and torsion angles; correlations between esds in cell parameters are only used when they are defined by crystal symmetry. An approximate (isotropic) treatment of cell esds is used for estimating esds involving l.s. planes.

Fractional atomic coordinates and isotropic or equivalent isotropic displacement parameters (\AA^2)

	<i>x</i>	<i>y</i>	<i>z</i>	$U_{\text{iso}}*/U_{\text{eq}}$
Zn1	0.500000	0.38978 (2)	0.750000	0.01617 (6)
N1	0.45636 (5)	0.28837 (11)	0.65132 (6)	0.01565 (17)
N2	0.55610 (6)	0.48063 (11)	0.67988 (6)	0.01854 (19)
C16	0.33235 (7)	0.14365 (15)	0.83074 (8)	0.0230 (2)
H16	0.341124	0.087836	0.877572	0.028*
C9	0.48444 (6)	0.22124 (13)	0.52702 (7)	0.0178 (2)
C1	0.49408 (6)	0.30237 (12)	0.59647 (7)	0.01542 (19)
C2	0.54576 (6)	0.40771 (12)	0.60987 (7)	0.0164 (2)
C8	0.52494 (7)	0.24688 (14)	0.47125 (8)	0.0227 (2)
H8	0.519116	0.190173	0.425081	0.027*
C10	0.43285 (7)	0.11731 (14)	0.51402 (8)	0.0217 (2)
H10	0.427219	0.059047	0.468550	0.026*
C7	0.57165 (7)	0.35008 (15)	0.48219 (8)	0.0232 (2)
H7	0.596684	0.366128	0.443013	0.028*
C6	0.58310 (7)	0.43410 (14)	0.55225 (8)	0.0199 (2)
C12	0.35616 (6)	0.19967 (13)	0.70258 (7)	0.0181 (2)
C15	0.28518 (7)	0.24956 (15)	0.82289 (8)	0.0237 (2)
C17	0.36714 (6)	0.11728 (14)	0.77154 (8)	0.0198 (2)
C11	0.39151 (7)	0.09962 (14)	0.56519 (8)	0.0219 (2)
H11	0.356957	0.031157	0.554933	0.026*
C20	0.41803 (7)	0.00090 (15)	0.78396 (9)	0.0250 (3)
H20A	0.463242	0.031778	0.816536	0.038*
H20B	0.422293	-0.031172	0.731288	0.038*
H20C	0.401508	-0.073317	0.812099	0.038*
C14	0.27287 (7)	0.32946 (15)	0.75349 (8)	0.0237 (2)
H14	0.240393	0.401532	0.746658	0.028*
C19	0.24812 (8)	0.27744 (19)	0.88737 (10)	0.0329 (3)
H19A	0.204988	0.225380	0.875753	0.049*
H19B	0.237646	0.374471	0.887957	0.049*
H19C	0.277652	0.250591	0.940294	0.049*
C13	0.30729 (6)	0.30568 (14)	0.69395 (8)	0.0212 (2)
C4	0.64006 (8)	0.61577 (16)	0.63859 (9)	0.0272 (3)
H4	0.672060	0.688821	0.649815	0.033*
C3	0.60226 (7)	0.58083 (14)	0.69353 (8)	0.0240 (2)
H3	0.609776	0.630540	0.742618	0.029*
C18	0.29227 (8)	0.39485 (18)	0.61986 (10)	0.0322 (3)
H18A	0.333702	0.447143	0.619199	0.048*
H18B	0.254432	0.457120	0.621039	0.048*
H18C	0.278912	0.338272	0.571181	0.048*

C5	0.63028 (7)	0.54297 (15)	0.56807 (9)	0.0251 (3)
H5	0.655364	0.566043	0.529928	0.030*
B1	0.40171 (7)	0.19187 (14)	0.63937 (8)	0.0171 (2)

Atomic displacement parameters (\AA^2)

	U^{11}	U^{22}	U^{33}	U^{12}	U^{13}	U^{23}
Zn1	0.01813 (9)	0.01939 (10)	0.01154 (8)	0.000	0.00488 (6)	0.000
N1	0.0160 (4)	0.0186 (4)	0.0133 (4)	0.0000 (3)	0.0055 (3)	0.0000 (3)
N2	0.0198 (5)	0.0209 (5)	0.0147 (4)	-0.0022 (4)	0.0042 (4)	0.0009 (3)
C16	0.0220 (6)	0.0303 (7)	0.0188 (5)	-0.0055 (5)	0.0089 (4)	0.0010 (5)
C9	0.0203 (5)	0.0193 (5)	0.0149 (5)	0.0015 (4)	0.0066 (4)	-0.0002 (4)
C1	0.0162 (5)	0.0178 (5)	0.0129 (4)	0.0023 (4)	0.0050 (4)	0.0016 (4)
C2	0.0167 (5)	0.0190 (5)	0.0139 (4)	0.0009 (4)	0.0048 (4)	0.0022 (4)
C8	0.0288 (6)	0.0247 (6)	0.0177 (5)	0.0025 (5)	0.0115 (5)	-0.0008 (4)
C10	0.0274 (6)	0.0212 (6)	0.0171 (5)	-0.0016 (5)	0.0070 (4)	-0.0034 (4)
C7	0.0266 (6)	0.0275 (6)	0.0194 (5)	0.0018 (5)	0.0127 (5)	0.0021 (5)
C6	0.0202 (5)	0.0227 (5)	0.0187 (5)	0.0006 (4)	0.0084 (4)	0.0046 (4)
C12	0.0152 (5)	0.0226 (6)	0.0169 (5)	-0.0034 (4)	0.0049 (4)	-0.0004 (4)
C15	0.0207 (5)	0.0314 (7)	0.0217 (6)	-0.0064 (5)	0.0105 (5)	-0.0050 (5)
C17	0.0174 (5)	0.0237 (6)	0.0192 (5)	-0.0038 (4)	0.0064 (4)	0.0015 (4)
C11	0.0233 (6)	0.0226 (6)	0.0203 (5)	-0.0049 (4)	0.0063 (4)	-0.0026 (4)
C20	0.0254 (6)	0.0256 (6)	0.0258 (6)	0.0007 (5)	0.0098 (5)	0.0059 (5)
C14	0.0183 (5)	0.0282 (7)	0.0265 (6)	-0.0010 (5)	0.0094 (5)	-0.0030 (5)
C19	0.0312 (7)	0.0431 (9)	0.0307 (7)	-0.0054 (6)	0.0191 (6)	-0.0066 (6)
C13	0.0179 (5)	0.0260 (6)	0.0209 (5)	-0.0004 (4)	0.0073 (4)	0.0016 (4)
C4	0.0264 (6)	0.0291 (7)	0.0260 (6)	-0.0084 (5)	0.0068 (5)	0.0041 (5)
C3	0.0266 (6)	0.0245 (6)	0.0195 (5)	-0.0064 (5)	0.0037 (5)	0.0006 (4)
C18	0.0294 (7)	0.0395 (8)	0.0309 (7)	0.0123 (6)	0.0137 (6)	0.0122 (6)
C5	0.0238 (6)	0.0293 (7)	0.0244 (6)	-0.0036 (5)	0.0100 (5)	0.0059 (5)
B1	0.0167 (5)	0.0197 (6)	0.0152 (5)	-0.0004 (4)	0.0045 (4)	0.0004 (4)

Geometric parameters (\AA , $^\circ$)

Zn1—N1 ⁱ	1.9606 (10)	C12—C13	1.4134 (18)
Zn1—N1	1.9606 (10)	C12—B1	1.5896 (18)
Zn1—N2	2.0527 (10)	C15—C14	1.393 (2)
Zn1—N2 ⁱ	2.0527 (10)	C15—C19	1.5080 (19)
N1—C1	1.3580 (14)	C17—C20	1.5127 (19)
N1—B1	1.4245 (17)	C11—H11	0.9500
N2—C2	1.3660 (16)	C11—B1	1.5315 (19)
N2—C3	1.3316 (17)	C20—H20A	0.9800
C16—H16	0.9500	C20—H20B	0.9800
C16—C15	1.391 (2)	C20—H20C	0.9800
C16—C17	1.3966 (18)	C14—H14	0.9500
C9—C1	1.4035 (16)	C14—C13	1.3920 (18)
C9—C8	1.4281 (17)	C19—H19A	0.9800
C9—C10	1.4310 (18)	C19—H19B	0.9800

C1—C2	1.4421 (17)	C19—H19C	0.9800
C2—C6	1.4095 (16)	C13—C18	1.507 (2)
C8—H8	0.9500	C4—H4	0.9500
C8—C7	1.362 (2)	C4—C3	1.3964 (19)
C10—H10	0.9500	C4—C5	1.374 (2)
C10—C11	1.3652 (18)	C3—H3	0.9500
C7—H7	0.9500	C18—H18A	0.9800
C7—C6	1.4257 (19)	C18—H18B	0.9800
C6—C5	1.4092 (19)	C18—H18C	0.9800
C12—C17	1.4020 (17)	C5—H5	0.9500
N1 ⁱ —Zn1—N1	118.68 (6)	C16—C17—C12	120.32 (12)
N1 ⁱ —Zn1—N2 ⁱ	84.72 (4)	C16—C17—C20	119.04 (12)
N1 ⁱ —Zn1—N2	122.48 (4)	C12—C17—C20	120.62 (11)
N1—Zn1—N2 ⁱ	122.48 (4)	C10—C11—H11	120.5
N1—Zn1—N2	84.72 (4)	C10—C11—B1	118.97 (12)
N2—Zn1—N2 ⁱ	128.26 (6)	B1—C11—H11	120.5
C1—N1—Zn1	109.89 (8)	C17—C20—H20A	109.5
C1—N1—B1	120.99 (10)	C17—C20—H20B	109.5
B1—N1—Zn1	128.11 (8)	C17—C20—H20C	109.5
C2—N2—Zn1	107.62 (8)	H20A—C20—H20B	109.5
C3—N2—Zn1	133.06 (9)	H20A—C20—H20C	109.5
C3—N2—C2	118.90 (11)	H20B—C20—H20C	109.5
C15—C16—H16	119.2	C15—C14—H14	119.4
C15—C16—C17	121.69 (12)	C13—C14—C15	121.22 (13)
C17—C16—H16	119.2	C13—C14—H14	119.4
C1—C9—C8	119.26 (11)	C15—C19—H19A	109.5
C1—C9—C10	118.26 (11)	C15—C19—H19B	109.5
C8—C9—C10	122.46 (11)	C15—C19—H19C	109.5
N1—C1—C9	123.33 (11)	H19A—C19—H19B	109.5
N1—C1—C2	118.03 (10)	H19A—C19—H19C	109.5
C9—C1—C2	118.63 (10)	H19B—C19—H19C	109.5
N2—C2—C1	117.15 (10)	C12—C13—C18	119.97 (11)
N2—C2—C6	122.03 (11)	C14—C13—C12	120.70 (12)
C6—C2—C1	120.82 (11)	C14—C13—C18	119.32 (12)
C9—C8—H8	119.0	C3—C4—H4	120.5
C7—C8—C9	122.07 (12)	C5—C4—H4	120.5
C7—C8—H8	119.0	C5—C4—C3	119.03 (13)
C9—C10—H10	119.1	N2—C3—C4	122.63 (13)
C11—C10—C9	121.79 (12)	N2—C3—H3	118.7
C11—C10—H10	119.1	C4—C3—H3	118.7
C8—C7—H7	119.9	C13—C18—H18A	109.5
C8—C7—C6	120.21 (11)	C13—C18—H18B	109.5
C6—C7—H7	119.9	C13—C18—H18C	109.5
C2—C6—C7	118.90 (12)	H18A—C18—H18B	109.5
C5—C6—C2	117.29 (12)	H18A—C18—H18C	109.5
C5—C6—C7	123.81 (12)	H18B—C18—H18C	109.5
C17—C12—C13	117.92 (11)	C6—C5—H5	120.0

C17—C12—B1	123.59 (11)	C4—C5—C6	120.08 (12)
C13—C12—B1	118.06 (11)	C4—C5—H5	120.0
C16—C15—C14	118.10 (12)	N1—B1—C12	115.27 (11)
C16—C15—C19	121.23 (13)	N1—B1—C11	116.51 (11)
C14—C15—C19	120.67 (14)	C11—B1—C12	128.12 (11)
Zn1—N1—C1—C9	166.76 (9)	C10—C9—C1—C2	-179.75 (11)
Zn1—N1—C1—C2	-14.38 (13)	C10—C9—C8—C7	176.87 (13)
Zn1—N1—B1—C12	20.10 (16)	C10—C11—B1—N1	-2.14 (19)
Zn1—N1—B1—C11	-163.25 (9)	C10—C11—B1—C12	174.00 (13)
Zn1—N2—C2—C1	7.93 (13)	C7—C6—C5—C4	-177.57 (14)
Zn1—N2—C2—C6	-172.71 (10)	C15—C16—C17—C12	1.2 (2)
Zn1—N2—C3—C4	172.48 (11)	C15—C16—C17—C20	179.74 (13)
N1—C1—C2—N2	4.08 (16)	C15—C14—C13—C12	-0.3 (2)
N1—C1—C2—C6	-175.29 (11)	C15—C14—C13—C18	180.00 (14)
N2—C2—C6—C7	177.35 (12)	C17—C16—C15—C14	0.4 (2)
N2—C2—C6—C5	-2.32 (19)	C17—C16—C15—C19	-179.75 (13)
C16—C15—C14—C13	-0.8 (2)	C17—C12—C13—C14	1.89 (19)
C9—C1—C2—N2	-177.01 (11)	C17—C12—C13—C18	-178.44 (13)
C9—C1—C2—C6	3.63 (17)	C17—C12—B1—N1	-96.44 (15)
C9—C8—C7—C6	2.0 (2)	C17—C12—B1—C11	87.37 (17)
C9—C10—C11—B1	-1.2 (2)	C19—C15—C14—C13	179.30 (13)
C1—N1—B1—C12	-172.61 (11)	C13—C12—C17—C16	-2.33 (18)
C1—N1—B1—C11	4.04 (17)	C13—C12—C17—C20	179.19 (12)
C1—C9—C8—C7	-1.7 (2)	C13—C12—B1—N1	75.93 (15)
C1—C9—C10—C11	2.81 (19)	C13—C12—B1—C11	-100.25 (16)
C1—C2—C6—C7	-3.32 (18)	C3—N2—C2—C1	-178.47 (11)
C1—C2—C6—C5	177.02 (12)	C3—N2—C2—C6	0.89 (18)
C2—N2—C3—C4	0.8 (2)	C3—C4—C5—C6	-0.5 (2)
C2—C6—C5—C4	2.1 (2)	C5—C4—C3—N2	-1.0 (2)
C8—C9—C1—N1	177.72 (11)	B1—N1—C1—C9	-2.63 (18)
C8—C9—C1—C2	-1.14 (17)	B1—N1—C1—C2	176.23 (11)
C8—C9—C10—C11	-175.75 (13)	B1—C12—C17—C16	170.06 (12)
C8—C7—C6—C2	0.5 (2)	B1—C12—C17—C20	-8.42 (19)
C8—C7—C6—C5	-179.86 (14)	B1—C12—C13—C14	-170.92 (12)
C10—C9—C1—N1	-0.89 (18)	B1—C12—C13—C18	8.75 (19)

Symmetry code: (i) $-x+1, y, -z+3/2$.